SPAWAR
Systems Center
PACIFIC

Technical Document 3275
September 2013

Silicon-on-Sapphire Waveguides for Widely Tunable Coherent Mid-IR Sources

Sanja Zlatanovic
Burton Neuner III
Bill Jacobs
Bruce Offord
Randy Shimabukuro

SSC Pacific

Space and Naval Warfare Systems Center Pacific
San Diego, CA 92152-5001

SSC Pacific
San Diego, California 92152-5001

J. J. Beel, CAPT, USN
Commanding Officer

C. A. Keeney
Executive Director

ADMINISTRATIVE INFORMATION

This project report was prepared by the Advanced Photonic Technologies Branch of the Enterprise Communications and Networks Division, Space and Naval Warfare Systems Center Pacific (SSC Pacific). The project is a part of the SSC Pacific In-House Science and Technology (S&T) Program and is funded by the Naval Innovative Science and Engineering Program as a Basic Research project.

Released by
Ayax Ramirez, Head
Advanced Photonic Technologies

Under authority of
Clark Hendrickson, Head
Enterprise Communications and Networks

EXECUTIVE SUMMARY

The goal of this project is to design and develop a widely tunable coherent light source in the wavelength range between 3 μm and 4 μm via four-wave mixing in silicon-on-sapphire waveguides. This project will address the Navy need to extend the range of spectrum dominance. Previous investigations have shown that this spectral range is of interest for applications that include free-space communications, laser radar, optical countermeasures, and remote sensing.

The project is a part of the Space and Naval Warfare Systems Center Pacific (SSC Pacific) In-House Science and Technology (S&T) Program and is funded by the Naval Innovative Science and Engineering Program as a Basic Research project.

This report summarizes the progress that has been made during fiscal year (FY) 2013 and it specifically includes

- A description of simulations and developed software that has been utilized for the design
- Waveguide designs
- The design and optimization of waveguide couplers
- The results of waveguide fabrication

CONTENTS

FIGURES

1. BACKGROUND

The mid-infrared (IR) range between 3 μm and 5 μm hosts an atmospheric transparency window, spectroscopic fingerprints of gases and molecules, and heat signatures. Consequently, it is an attractive spectral region for applications such as free-space optical communications, laser detection and ranging (laser radar), remote sensing, and optical countermeasures. All of these applications can benefit from the existence of agile (i.e., frequency and modulation) light sources. While the band beyond 4 μm is well covered by quantum cascade lasers, the band below 4 μm, despite recent progress in intraband cascade lasers, still presents a challenge due to limitations in material properties. Four-wave mixing processes have been utilized previously to generate new wavelengths by leveraging existing sources in telecom and short-wave infrared (SWIR) bands. It has been demonstrated using silicon waveguides on silicon-on-silicon dioxide that wavelengths beyond 2.2 μm can be generated using four-wave mixing [1, 2]. Recently, generation of 3.6-μm wavelength light has also been reported [3].

The approach proposed under this project involves the four-wave mixing of a pump at a SWIR wavelength around 2 μm and signals in the near-IR telecommunication band to generate light in the mid-IR (Figure 1). Pumping silicon at SWIR diminishes parasitic effects such as two-photon absorption that would be detrimental to four-wave mixing efficiency.

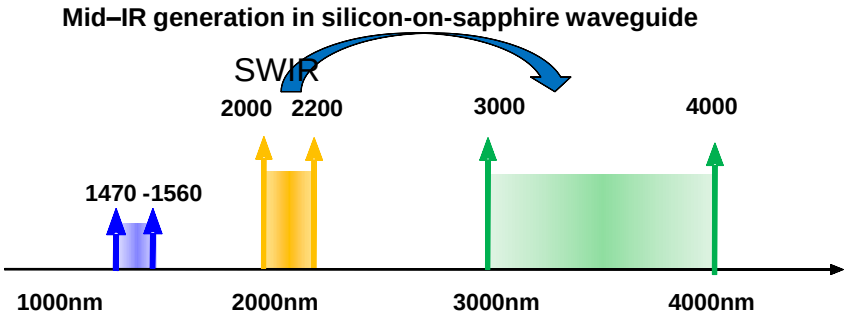

Figure 1. Approach: SWIR wavelength pumps and telecommunication band signals are utilized in a four-wave mixing process to generate mid-IR light from 3 μm to 4 μm.

Four-wave mixing is a good choice for generation of mid-IR wavelengths because it has the potential of combining the following properties in a single light source:

- Wide tunability in the 3-μm to 4-μm range
- Fast sweeping and wavelength hopping
- Data encoding capability
- Small size

Four-wave mixing allows the direct transfer of complex modulation formats from the telecommunication band to the mid-IR band. This is of great importance for free-space optical links in the mid-IR band since this band lacks devices that are required for high-speed optical communications. On the other hand, the telecommunication band around 1.5 μm has a great infrastructure that can be leveraged for communications in the mid-IR. The benefits to laser radar applications that this technology offers are based on wide tuning and fast sweeping that can allow adaptability to the environmental conditions and operation at wavelengths where environmental

effects are least detrimental. Infrared countermeasures can also benefit from wide tuning and fast sweeping.

Silicon waveguides are our platform of choice because they have good nonlinear characteristics. However, the silicon-on-silicon dioxide platform that has been used previously for generating longer wavelengths has limitations in that silicon dioxide substrates become non-transparent for wavelengths beyond 3.6 μm (Figure 2a). Therefore, we opted for a silicon-on-sapphire platform. Sapphire substrates show good transparency from visible wavelengths to 5 μm and are therefore a good choice for this application (Figure 2b).

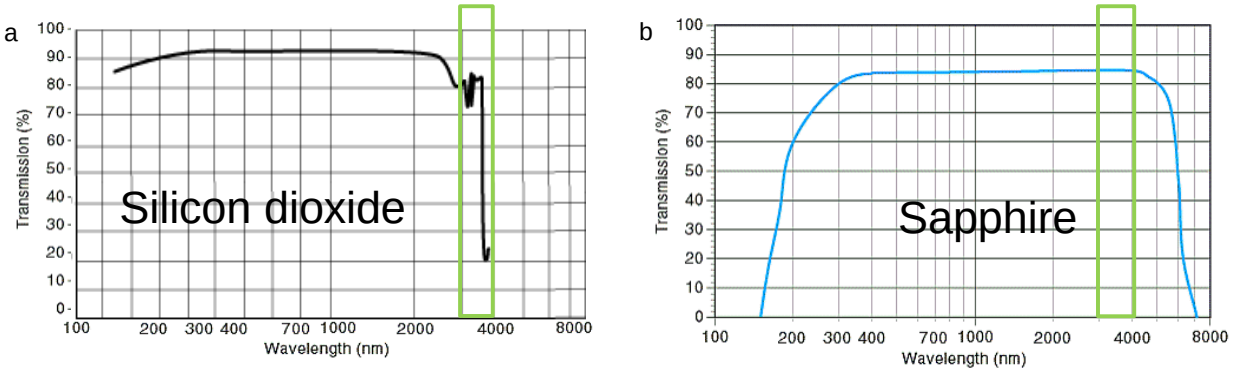

Figure 2. Transmission properties of silicon dioxide (a) and sapphire (b).

2. SIMULATIONS

Four-wave mixing is a nonlinear process that occurs in materials with large third-order nonlinear susceptibility, $\chi^{(3)}$, and results in a large Kerr coefficient, n_2. Silicon possesses a large Kerr coefficient on the order of $10^{-13}cm^2/W$. This coefficient is 150 times larger than that of silica glass. At the same time, silicon has very large index of refraction that provides great confinement of light in the silicon waveguides, creating very high light intensities. Intensity, along with Kerr coefficient, plays an important role in efficient generation of new wavelengths. During the four-wave mixing process, two photons from a high-power pump are annihilated and two photons are generated, one at the wavelength of the signal photon, and one at the new wavelength that is referred to as the idler wavelength. The wavelength of the idler photon is determined by energy conservation, and in terms of the corresponding frequencies, it is expressed as $\omega_i=2*\omega_p-\omega_s$, where ω_p and ω_s are frequencies of pump and signal, respectively. The efficiency of idler generation depends also on phase-matching that stems from momentum conservation and is expressed as $\Delta\beta=2\pi((n_s/\lambda_s)+ (n_i/\lambda_i)-2(n_p/\lambda_p))$, where n_s, n_i, and n_p are effective indices of refraction of silicon waveguide at signal, idler, and pump wavelengths, respectively. Phase-mismatch is a direct consequence of material and waveguide dispersion. In order to achieve efficient generation of idler wavelengths, phase-mismatch ($\Delta\beta$) needs to satisfy the following condition: $-4\gamma P_p<\Delta\beta<0$. Here, $\gamma=n_2\omega_0/(cA_{eff})$ is a nonlinear coefficient that is directly proportional to the Kerr coefficient and frequency, and inversely proportional to the modal area (A_{eff}) in the silicon waveguide and speed of light (c), and P_p is the pump power.

Since phase-mismatch is a direct consequence of dispersion properties of the nonlinear medium (in this case, silicon-on-sapphire waveguides), the capability to tailor and engineer the waveguide dispersion properties is key to the efficient generation of long wavelengths. Tailoring of dispersion can be achieved by changing the geometry of the waveguides as well as the cladding material. We conducted a number of simulations with the goal of identifying waveguide geometries for which the phase-matching condition $-4\gamma P_p<\Delta\beta<0$ is satisfied.

We considered two types of wafers that were available for purchase: one with a silicon thickness of 600 nm, and the other with a thickness of 280 nm. With the 280-nm-thick silicon, we were not able to find geometries to satisfy the phase-matching condition, but we did identify them for 600-nm-thick silicon-on-sapphire. The cladding for these waveguides is air on one side and sapphire on the other side, as shown in Figure 3, which represents the calculated mode for one of the waveguides.

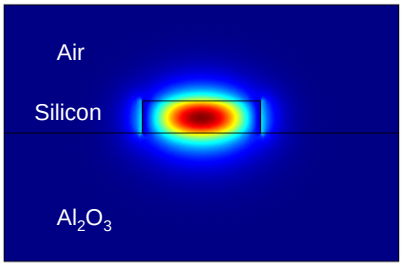

Figure 3. Mode profile of the silicon waveguide with air cladding above and sapphire cladding below.

2.1 WAVEGUIDE DISPERSION

Finite element method software (COMSOL®) was used to calculate effective indices of the waveguides at wavelengths ranging from 1.2 μm to 4 μm. An example of waveguide refractive index dispersion is given in Figure 4 for a waveguide of 600-nm height and 1.6-μm width.

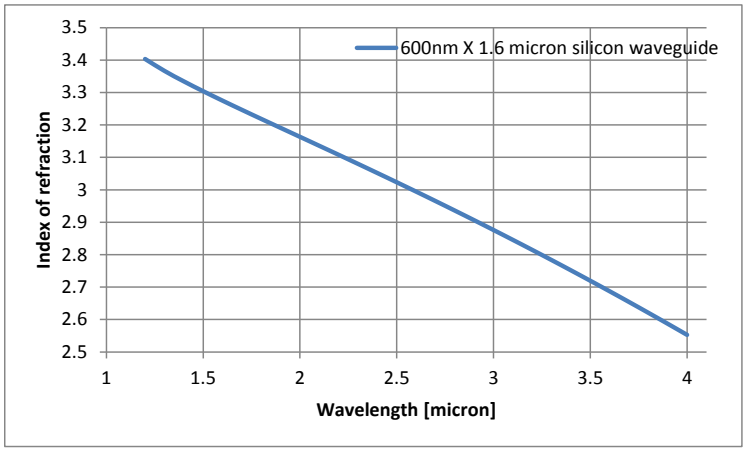

Figure 4. Effective index of refraction dispersion for silicon-on-sapphire waveguides.

From effective indices, we can calculate phase mismatch (Δβ) for a range of signal and pump wavelengths. If developed into a Taylor expansion, Δβ can be approximated as $\Delta\beta = \beta^{(2)}(\Delta\omega)^2 + \beta^{(4)}(\Delta\omega)^4/12$ using two coefficients $\beta^{(2)}$ and $\beta^{(4)}$ that describe the shape of the phase-mismatch curve, and Δω that represents the difference between pump and signal frequencies. When looking at the shapes of the curve, and keeping in mind the condition that phase-mismatch must satisfy and that we would like to generate frequencies (wavelengths) that are very distant from the pump, we conclude that the best option is to design the waveguides with $\beta^{(2)} > 0$ and $\beta^{(4)} < 0$ (Figure 5). As can be seen from the shaded region in Figure 5 (with the conditions mentioned above), phase-matching occurs at wavelengths far away from the pump. This has an advantage compared to other $\beta^{(2)}$, $\beta^{(4)}$ combinations in that it reduces noise at wavelengths close to the pumps.

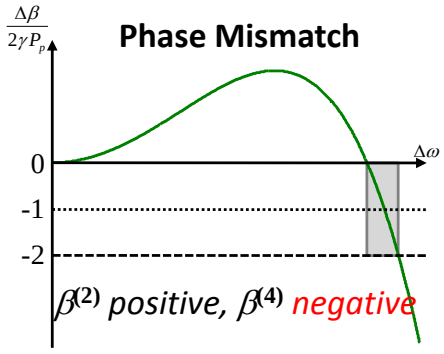

Figure 5. Phase-matching condition: efficient generation occurs at frequencies distant from the pump for which the phase-mismatch overlaps the shaded region.

According to our simulations, dispersion of silicon waveguides with 600-nm height shows positive $\beta^{(2)}$ and negative $\beta^{(4)}$, and therefore we were able to identify waveguides that have low phase-mismatch in the wavelength range between 3 μm and 4 μm.

To calculate wavelengths that can be efficiently generated, we utilized a Matlab code that sweeps through the range of signal and pump wavelengths and calculates gain using phase-mismatch and pump power as follows:

$$G = 1 + \left(\frac{\gamma P_p}{g}\right)^2 \sinh^2(gL),$$

where L is waveguide length, and $g = \sqrt{\left(\gamma P_p\right)^2 - \left(\left(\Delta\beta + 2\gamma P_p\right)/2\right)^2}$ [4].

Based on these equations, we obtained gain plots for different waveguides (Figure 6). As can be observed in the figure, there are two branches for which high gain is achieved. One belongs to the signal and the other to the idler wavelength. It can be seen that for the chosen pump power of 1W and waveguide length of 2.5 cm, gain in excess of 6 dB can be obtained, as indicated by the color bar. This means that idler power can, in theory, be 4 times higher than the power of the initial signal that seeds the four-wave mixing process. These simulations assume that linear loss in the waveguides is minimal. Waveguide losses will depend on the fabrication process and on the smoothness of waveguide walls. In addition, it can be seen that when the waveguide width increases, the required pump tuning range moves to longer wavelength. Consequently, by fabricating the waveguides at range of widths from 1.5 μm to 2.5 μm, we assure that some of them will fall into the working range of the tunable SWIR pump source. It can also be observed from the graphs that when the pump is tuned by approximately 70 nm, the idler can be tuned by 1 μm. As a result, the tuning speed is also increased by more than 10 times. For example, if the pump can be tuned with a speed of 70 nm/s, then the idler will be tuned with speed that is 13 times faster (1 μm/s).

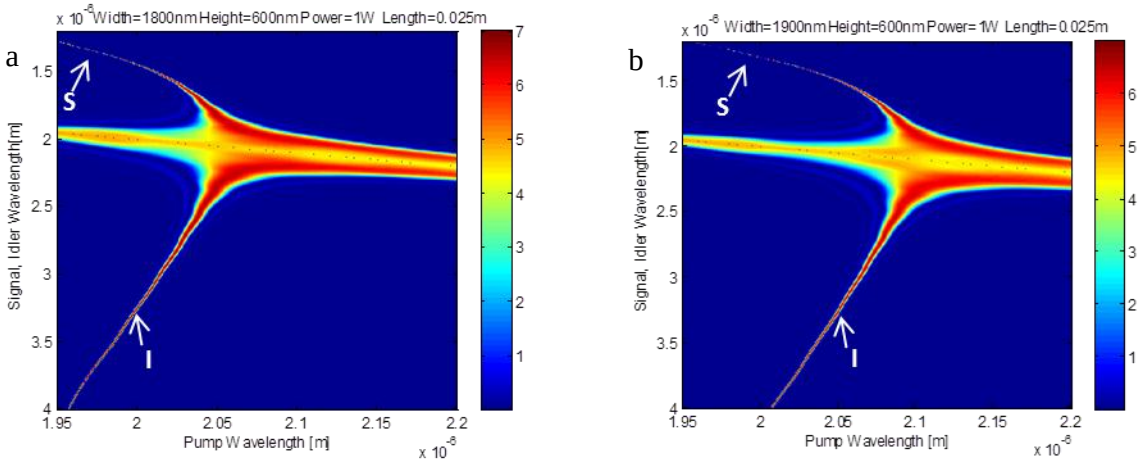

Figure 6. Graph of the signal and idler gain for a waveguide of 600-nm thickness and width of 1800 nm (a) and 1900 nm (b).

2.2 WAVEGUIDE COUPLERS

The efficiency of the four-wave mixing process increases approximately as a square of the pump power. High pump powers are therefore extremely important for the generation of power at longer wavelengths. Consequently, it is important that coupling loss into the waveguides is minimized. This is a well-known challenge for silicon photonics, since the mode inside the silicon waveguide is highly confined compared to the modes in silica fiber. In order to couple light from fiber into the silicon waveguides, we use tapered, lensed fibers. On the silicon side, we considered a number of coupler geometries (Figure 7) and calculated their coupling efficiency using 3D Finite Difference Time Domain (FDTD) modeling. In the simulations, we considered spot size generated by the tapered lensed fiber to be 2.5 μm, which corresponds to values reported by the manufacturer.

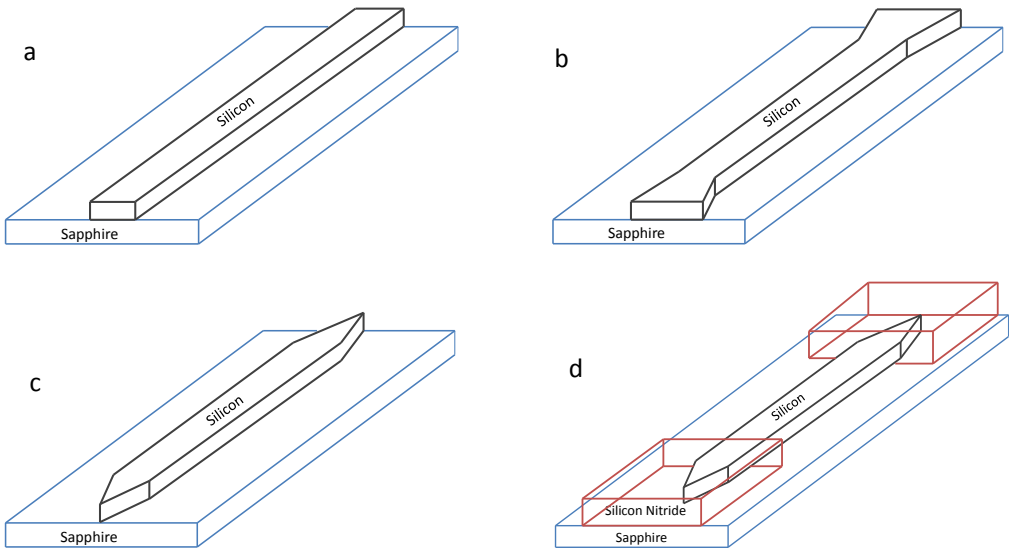

Figure 7. Waveguide couplers: (a) flat coupler, (b) tapered coupler, (c) spot size converter (inverse taper), (d) spot size converter with SiN waveguide overlay.

Flat couplers (Figure 7a) consisted of 2-μm-wide and 600-nm-tall silicon-on-sapphire waveguides with air cladding on top. According to the simulation, these couplers would ideally have a coupling efficiency of ~56%. Tapered couplers (Figure 7b) have wider front facets 5-μm wide and 600-nm tall, and show a slightly better coupling efficiency of 65%. During fabrication, it is critical that facets of these couplers are well-polished, so that there is no additional loss as a result of scattering from the rough surface.

Inverse tapers or spot size converters (Figure 7c) were simulated with air cladding on top as well as with SiN cladding. The tip of an inverse taper had width of 100 nm, and the length of the taper is 100 μm. In the case of air cladding, the transverse electric (TE) mode cannot be coupled into the waveguide efficiently, while the transverse magnetic (TM) mode couples with efficiency of 45%. Therefore, because of the poor performance, these couplers are not suitable for our application. When SiN serves as a cladding, coupling efficiency drastically increases to more than 75% for both TE and TM modes.

Ultimately, if another waveguide made from SiN is fabricated on top of the inverse taper (Figure 7d), the coupling efficiency increases to 88% for both TE and TM modes. The dimensions of the SiN waveguide in this case were 4-μm width and 2-μm height. These couplers show a very good performance in simulations. An example of the simulation results is given in Figure 8. While the fabrication process for the flat and tapered couplers is straightforward and can be done using photolithography, the fabrication of the spot size converters with SiN waveguides requires multiple additional fabrication steps and e-beam lithography.

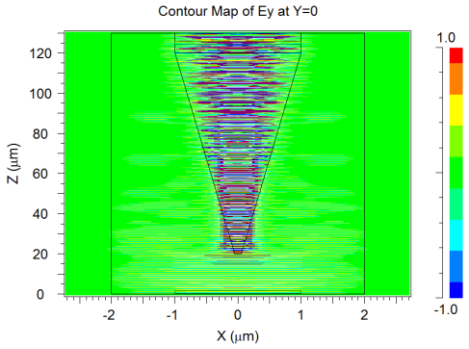

Figure 8. FDTD simulation showing light coupling (TM mode) into a spot size converter with a SiN waveguide: the electric field in the center of the silicon waveguide.

3. FABRICATION

Standard, commercially available SOS wafers with 0.6-µm silicon thickness were used as starting material for the waveguides. These SOS wafers were not treated using a solid phase epitaxial process, so the silicon has a high concentration of crystalline (twinning) defects in the first 300 nm of thickness due to the lattice mismatch between sapphire and silicon. The optically defined silicon waveguides were fabricated on 1”X1” pieces diced from the SOS wafers. Standard lithography using a 1X contact mask was used to fabricate the waveguides on the 600-nm-thick silicon layer with a sapphire substrate of 500-µm thickness. Figure 9 shows the 1X mask layout. Blue lines on the mask represent silicon waveguides. The length of the waveguides ranged from 10 mm to 30 mm, and widths ranged from 1.5 µm to 2.5 µm. Green lines on the mask are SiN waveguide overlays, used with spot size converters. As previously shown, the couplers with SiN waveguide overlays show optimal coupling efficiency, and a process was developed to deposit and pattern silicon nitride onto the waveguides. Since silicon and nitride both etch at similar rates, a patterned oxide was used to preserve the silicon waveguides from the nitride dry-etch, and this SiO_2 protective layer is represented by a red pattern on the mask.

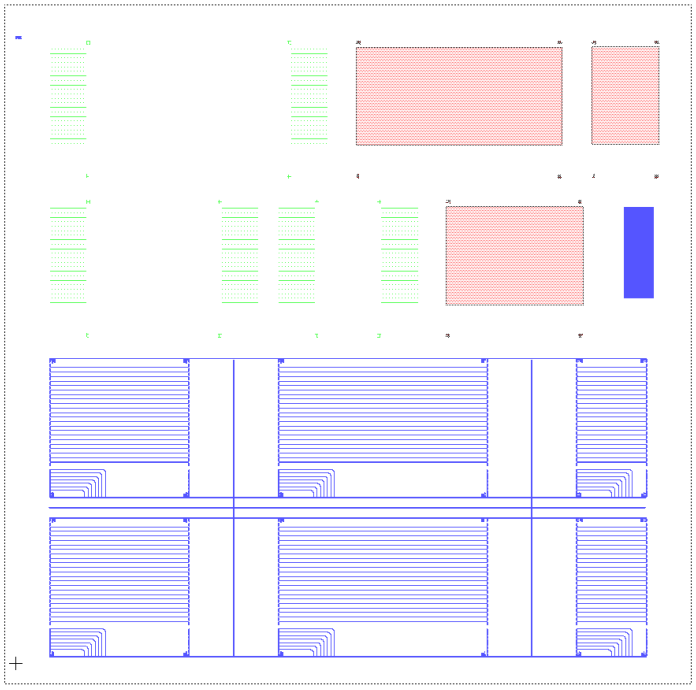

Figure 9. Mask layout for the 1X optical contact mask.

3.1 FABRICATION STEPS

The silicon waveguide fabrication process consists of the following steps. After cleaning and air drying, the dies were soaked in a hexamethyldisilazane (HMDS) bath for 2 minutes that served as a primer. Next, Shipley S1805 photoresist was spin-coated at 5000 rpm for 40 s with a ramp of 250 rpm/s. The samples were baked for 90 s on a hot plate at 115^{o}C. The samples were exposed using the Karl Suss MA6 mask aligner at 365 nm and intensity of 11 mW/cm^2. Exposure times were calibrated

by examining samples with exposure time from 1.5 s to 3.5 s. While the samples with exposure times of 3.5 s have shown evidence of overexposure, such as rounded edges, samples with exposure times of 1.5 s gave the best results. Some edge rounding is still present with this shorter exposure time, so we are considering lowering it further in future tests.

In the next step, the photoresist was developed in MF 319 by lightly moving our sample around the developer solution for 45 s and immediately dipping it in deionized water to stop the developing process. Developing was followed by a hard bake at 115^{o}C for 5 minutes.

The waveguides were etched on the Plasma Lab p100 reactive ion etcher using the following recipe: 50 sccm of C4F8 and 25 sccm of SF6 at 30W RF and 1200W ICP, at a pressure of 15 mtorr and 20 ^{o}C. The approximate material removal rate was 500 nm/min, and an etching time of 80 s provided optimal results.

A PE IIB Planar etcher at 200 mtorr of O_2 under 200 W of power was used to descum the samples. Since there is still some residual photoresist after 4 minutes, the process needs to be recalibrated. This step completes the fabrication of silicon waveguides.

The spot size converters with SiN overlays require additional fabrication steps, as shown in Figure 10. Following patterning and etching of silicon waveguides, a SiO_2 protective layer is deposited on top of the waveguides and is patterned using a photolithographic mask. The sample is then etched. Next, the SiN layer of 2-micron thickness is deposited on top, patterned, and etched. Finally, the SiO_2 protective layer is removed, leaving waveguides with the couplers. This fabrication is a work in progress.

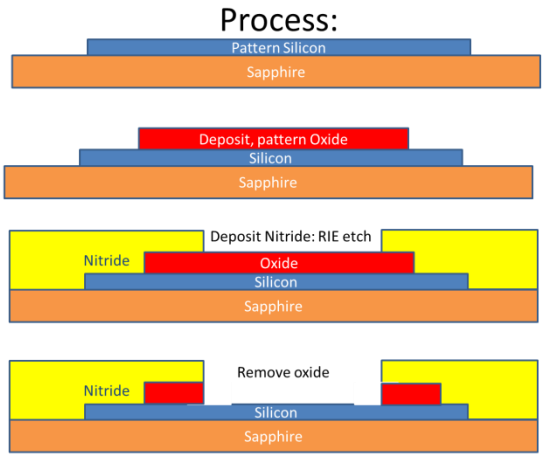

Figure 10. Process sequence for nitride cladding of waveguides.

3.2 FABRICATION RESULTS

The SEM images of some of the fabricated waveguides are shown in Figure 11. The first waveguide prototypes were fabricated at San Diego State University using 180-nm-thick silicon bonded to sapphire substrate (Figure11a). In this prototype, due to limited resources, a plastic transparency mask with a feature size of 5μm was used for patterning, resulting in waveguide roughness. Waveguide roughness is the main cause of propagation loss and must be minimized. Figures 11b and c show waveguides patterned using chrome on a glass mask with address size of 50

nm. These waveguides were fabricated at the University of California, La Jolla Nano3 facility. They show roughness with sub-100-nm features.

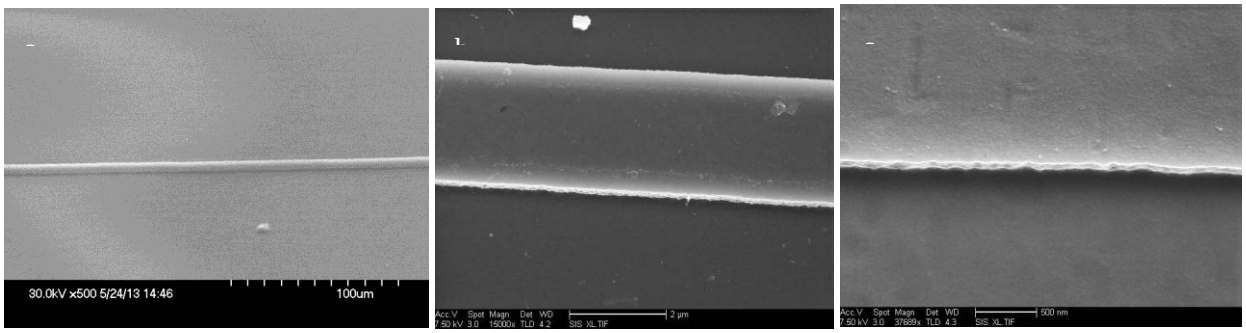

Figure 11. SEM of fabricated waveguides: (a) waveguides fabricated using a transparency mask; (b), (c) waveguides fabricated using a chrome mask.

While waveguides fabricated using a chrome mask show lower roughness, we expect that it will further be reduced using e-beam patterning.

4. CONCLUSION

The silicon-on-sapphire waveguide is a promising candidate for the generation of mid-IR light using four-wave mixing. We identified the cross-sectional geometries of silicon waveguides that satisfy phase-matching condition and should allow efficient generation of mid-IR light. The couplers for efficient coupling of light from tapered fibers into the waveguides were designed. Two geometries were chosen: regular tapers on silicon waveguides, and spot-size converters composed of large SiN waveguides overlaying inverse tapers on the silicon waveguides. The waveguides with regular tapers were fabricated using photolithography. To test the waveguides, some post-processing, such as cleaving and polishing facets, needs to be completed. Inverse-tapered silicon waveguides were fabricated using e-beam lithography. Future work will include the deposition and pattering of SiN to incorporate larger overlaying waveguides required for efficient coupling. We plan to conduct measurements of propagation and coupling losses in the waveguides, and four-wave mixing experiments to generate mid-IR light.

5. REFERENCES

[1] Zlatanovic, Sanja, et al. "Mid-infrared wavelength conversion in silicon waveguides using ultracompact telecom-band-derived pump source." *Nature Photonics* 4.8 (2010): 561-564.

[2] Liu, Xiaoping, et al. "Mid-infrared optical parametric amplifier using silicon nanophotonic waveguides." *Nature Photonics* 4.8 (2010): 557-560.

[3] Kuyken, Bart, et al. "Mid-infrared generation by frequency down-conversion across 1.2 octaves in a normally-dispersive silicon wire." *CLEO: Science and Innovations*. Optical Society of America, 2013.

[4] Agrawal, Govind P. “Nonlinear fiber optics.” Springer Berlin Heidelberg, 2000.

REPORT DOCUMENTATION PAGE

Form Approved
OMB No. 0704-01-0188

PLEASE DO NOT RETURN YOUR FORM TO THE ABOVE ADDRESS.

1. REPORT DATE *(DD-MM-YYYY)*	2. REPORT TYPE	3. DATES COVERED *(From - To)*
09–2013	Final	

4. TITLE AND SUBTITLE

Silicon-on-Sapphire Waveguides for Widely Tunable Coherent Mid-IR Sources

5a. CONTRACT NUMBER

5b. GRANT NUMBER

5c. PROGRAM ELEMENT NUMBER

6. AUTHORS

Sanja Zlatanovic
Burton Neuner III
Bill Jacobs
Bruce Offord
Randy Shimabukuro

5d. PROJECT NUMBER

5e. TASK NUMBER

5f. WORK UNIT NUMBER

7. PERFORMING ORGANIZATION NAME(S) AND ADDRESS(ES)

Space and Naval Warfare Systems Center Pacific (SSC Pacific)
San Diego, CA 92152–5001

8. PERFORMING ORGANIZATION REPORT NUMBER

TD 3275

9. SPONSORING/MONITORING AGENCY NAME(S) AND ADDRESS(ES)

Space and Naval Warfare Systems Center Pacific (SSC Pacific)
San Diego, CA 92152–5001

10. SPONSOR/MONITOR'S ACRONYM(S)

SSC Pacific

11. SPONSOR/MONITOR'S REPORT NUMBER(S)

12. DISTRIBUTION/AVAILABILITY STATEMENT

Approved for public release.

13. SUPPLEMENTARY NOTES

14. ABSTRACT

The goal of this project is to design and develop a widely tunable coherent light source in the wavelength range between 3 μm and 4 μm via four-wave mixing in silicon-on-sapphire waveguides. This project will address the Navy need to extend the range of spectrum dominance. Previous investigations have shown that this spectral range is of interest for applications that include free-space communications, laser radar, optical countermeasures, and remote sensing. The project is a part of the Space and Naval Warfare Systems Center Pacific (SSC Pacific) In House S&T Program and is funded by the Naval Innovative Science and Engineering Program as a Basic Research project. This report summarizes the progress that has been made during fiscal year (FY) 2013 and it specifically includes

- A description of simulations and developed software that has been utilized for the design
- Waveguide designs
- The design and optimization of waveguide couplers
- The results of waveguide fabrication

15. SUBJECT TERMS

Mission Area: Communications
Widely Tunable Coherent Mid-IR Sources; silicon-on-sapphire waveguides

16. SECURITY CLASSIFICATION OF:			17. LIMITATION OF ABSTRACT	18. NUMBER OF PAGES	19a. NAME OF RESPONSIBLE PERSON
a. REPORT	b. ABSTRACT	c. THIS PAGE			S. Zlatanovic
U	U	U	U		19B. TELEPHONE NUMBER *(Include area code)* (619) 767–4078

INITIAL DISTRIBUTION

853	Archive/Stock	(1)
843	Library	(2)
55360	S. Zlatanovic	(1)

Defense Technical Information Center
Fort Belvoir, VA 22060–6218 (1)

Approved for public release.

Space and Naval Warfare Systems Center Pacific
San Diego, CA 92152-5001